Proc. Natl. Acad. Sci. USA
Vol. 95, pp. 4748–4753, April 1998
Physiology

Cardiac arrest in rodents: Maximal duration compatible with a recovery of neuronal activity

S. CHARPAK*† AND E. AUDINAT‡

*Laboratory of Physiology and ‡Laboratory of Neurobiology, Centre National de la Recherche Scientifique, Unité Mixte de Recherche 7637, Ecole Supérieure de Physique et de Chimie Industrielles, 10 rue Vauquelin, 75005, Paris, France

Communicated by Jean Dausset, Centre d'Etude du Polymorphisme Humain, Paris, France, February 12, 1998 (received for review December 8, 1997)

ABSTRACT **We report here that during a permanent cardiac arrest, rodent brain tissue is "physiologically" preserved *in situ* in a particular quiescent state. This state is characterized by the absence of electrical activity and by a critical period of 5–6 hr during which brain tissue can be reactivated upon restoration of a simple energy (glucose/oxygen) supply. In rat brain slices prepared 1–6 hr after cardiac arrest and maintained *in vitro* for several hours, cells with normal morphological features, intrinsic membrane properties, and spontaneous synaptic activity were recorded from various brain regions. In addition to functional membrane channels, these neurons expressed mRNA, as revealed by single-cell reverse transcription–PCR, and could synthesize proteins *de novo*. Slices prepared after longer delays did not recover. In a guinea pig isolated whole-brain preparation that was cannulated and perfused with oxygenated saline 1–2 hr after cardiac arrest, cell activity and functional long-range synaptic connections could be restored although the electroencephalogram remained isoelectric. Perfusion of the isolated brain with the γ-aminobutyric acid A receptor antagonist picrotoxin, however, could induce self-sustained temporal lobe epilepsy. Thus, in rodents, the duration of cardiac arrest compatible with a short-term recovery of neuronal activity is much longer than previously expected. The analysis of the parameters that regulate this duration may bring new insights into the prevention of postischemic damages.**

Cardiac arrest lasting a few seconds to a couple of minutes can be reversed without brain damage upon cardiopulmonary resuscitation. After cardiac arrests lasting longer, however, reperfusion of the brain is accompanied by delayed irreversible brain damage that occurs several days after reperfusion of the tissue (for reviews, see refs. 1 and 2). The postischemic period during which neuronal activity recovers but which precedes the appearance of delayed damage is particularly important because it constitutes a therapeutic window in which to prevent delayed cell death. In animal models of global normothermic ischemia, it has been shown that this postischemic period occurs even after a complete interruption of cerebral blood flow lasting up to 1 hr (3–6). Our purpose here was to evaluate the maximal duration of cardiac arrest compatible with the occurrence of this postischemic period. The early phase of the period was analyzed in acute brain tissue prepared after a cardiac arrest of several hours and maintained *in vitro*.

Criteria characterizing acute tissue health *in vitro* are not clearly established (7). However, the association of normal electrophysiological and morphological parameters with the presence of undegraded mRNAs and the ability of the *in vitro* tissue to synthesize proteins should constitute an ensemble of signs representative of good health. Furthermore, the evolution of these parameters as a function of the delay between cardiac arrest and brain tissue reoxygenation should reflect the ability of the tissue to recover. Our results demonstrate that during a prolonged cardiac arrest in conditions where temperature declines normally, brain tissue is kept for hours in a particular state that is partially reversible upon reoxygenation.

METHODS

Slice Preparation and Recordings. Standard brain slices were prepared from young (15- to 35-day-old) and adult rats anesthetized with a mixture of ketamine and xylazine (100 mg/kg and 16 mg/kg, respectively). After decapitation and brain extraction, 400-μm-thick slices were cut at 4°C, incubated at room temperature (20–24°C) in a chamber containing oxygenated saline for 1 hr, and then placed in a submerged recording chamber maintained at 35°C. The standard extracellular oxygenated saline (95% O_2/5% CO_2) contained (in mM): 126 NaCl, 26 HCO_3, 15 glucose, 2.5 KCl, 1 $MgCl_2$, 1.25 NaH_2PO_4, 2 $CaCl_2$, and 5 pyruvate. These slices, prepared immediately after sacrificing the animal, were defined as standard slices, as opposed to postmortem (PM) slices, which are prepared as follows. Young (15- to 35-day-old) and adult rats (n = 45) were killed with an overdose of a ketamine/xylazine mixture, an overdose of pentobarbital, or by decapitation. Dead animals or heads were left on the bench for variable PM delays (1–12 hr), the brain cooling naturally to room temperature (20–24°C) in about 25 min. Time 0 of death was defined as the time of cardiac arrest observed by means of a thoracotomy. Coronal and parasagittal brain slices (n = 225) were cut at room temperature and left for at least 1 hr in a well containing the standard (20–24°C) oxygenated (95% O_2/5% CO_2) medium. Oxygenation of the medium was compulsory for tissue reactivation. In a series of experiments performed to quantify the effect of PM delay on tissue health, thick parasagittal slices of the primary olfactory cortex were cut to contain a large part of the lateral olfactory tract. In the recording chamber, neurons were visualized by using infrared videomicroscopy and recorded in the whole-cell mode with an Axopatch 200A amplifier (Axon Instruments). The patch pipette contained (in mM): 144 potassium gluconate, 3 $MgCl_2$, 0.2 EGTA, and 10 Hepes and 2 mg/ml biocytin or neurobiotin. Occasionally, 4 mM MgATP and 0.4 mM TrisGTP were added. Membrane potentials were corrected for the junction potential (−11 mV) and in current clamp experiments (Iclamp fast mode), the series resistance was not compensated. To study synaptic currents, CsCl was substituted for potassium gluconate in the patch pipette solution. Data acquisition and

The publication costs of this article were defrayed in part by page charge payment. This article must therefore be hereby marked "*advertisement*" in accordance with 18 U.S.C. §1734 solely to indicate this fact.

Abbreviations: PM, postmortem; RT-PCR, reverse transcription–PCR; GAD, glutamic acid decarboxylase; EEG, electroencephalogram; EPSP, excitatory postsynaptic potential; GABA, γ-aminobutyric acid.

†To whom reprint requests should be addressed. e-mail: serge.charpak@espci.fr.

analysis were performed with ACQUIS1 software (Gérard Sadoc, Gif/Yvette, France). Slices containing cells labeled with biocytin or neurobiotin were processed according to Horikawa and Armstrong (8), but revealed with ExtrAvidin coupled to fluorescein isothiocyanate (FITC) (1:200, Sigma). For some histological controls, 60-μm brain slices were stained with thionin.

Isolated Whole-Brain Preparation. We used the procedure described by Mühlethaler *et al.* (9), with some modifications. To avoid blood clotting, anesthetized guinea pigs (250–300 g) were perfused intracardially for 1–3 min with extracellular medium (room temperature), left on the bench for 1 hr, and then decapitated. The brain was extracted, placed in the recording chamber, and perfused through one vertebral artery or the basilar trunk with the medium slowly heated to 27–30°C. Leaking arteries were tied up. Extracellular stimulation was obtained by placing a bipolar electrode on the lateral olfactory tract. A tungsten electrode (1–5 MΩ) was used for field potential recordings. Current source density analysis (10) was implemented in a single dimension of the field potential profile. Intracellular recordings were performed with glass micropipettes containing 3 M KCl.

Single-Cell Reverse Transcription (RT)-PCR. At the end of whole-cell recordings from young rat slices, the cytoplasm was aspirated into the patch pipette and expelled with the autoclaved intracellular solution into a test tube where a reverse transcription was performed (11). This procedure was followed by a multiplex PCR amplification designed to amplify the mRNAs of glutamic acid decarboxylase (GAD_{65} and GAD_{67}) as described by Cauli *et al.* (12). The identity of the amplified DNA fragments was confirmed by Southern blot analysis.

c-Fos Activation. Hippocampal coronal slices from young rats were collected after a PM delay of 1 or 2 hr and left at room temperature for at least 1 hr in a well containing standard oxygenated solution (see above). Slices were then incubated for 3 hr in oxygenated, heated wells (35°C) containing the standard solution either alone or supplemented with 10/20 μM kainate, 10/20 μM kainate and 20 μM bicuculline, or 50 mM K^+ (NaCl was reduced to maintain a constant osmolarity). Slices were then fixed and processed (13) with a sheep polyclonal antibody to Fos oncoproteins (1:1000; Genosys, The Woodlands, TX). Actinomycin D (5 μM) and cycloheximide (35 μM) were applied at 35°C 1 hr before and during slice stimulation.

RESULTS

The general aspect of PM slices (see *Methods* for definition), obtained from rats killed with an overdose of ketamine/xylazine (n = 45), pentobarbital (n = 6), or by decapitation (n = 6), was first analyzed with infrared videomicroscopy. Cells from neocortical, hippocampal, cerebellar, and thalamic slices prepared after a PM delay of 1 hr and reoxygenated for 1 hr displayed a "normal, healthy" aspect. The ability of slices to recover from a PM delay of increasing duration is illustrated in Fig. 1. In blind experiments, standard (PM delay 0) and PM cortical slices were indistinguishable as long as the PM delay lasted less than 5 hr. Longer delays dramatically decreased the ability of slices to recover (Fig. 1, PM delay 7). Moreover, no difference was noticed between PM slices obtained from animals killed with ketamine/xylazine, pentobarbital, or decapitation, and therefore the data were pooled. It should be emphasized that dead animals were left to cool to room temperature during the PM delay, to mimic the natural conditions of a cardiac arrest, but it was noticed that the slice viability decreased when the body was artificially maintained at 34°C.

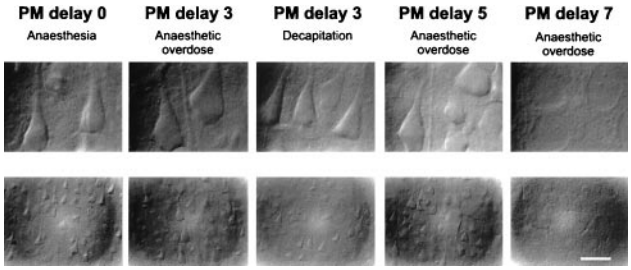

FIG. 1. Layer V pyramidal cells from neocortical slices prepared after various PM delays and visualized with infrared videomicroscopy. Cell morphology was observed with Nomarski optics at high (*Upper*) and low (*Lower*) magnifications (calibration bar = 17.5 and 70 μm, respectively). Experimental conditions from left to right: standard slice (PM delay 0); slice prepared after a PM delay of 3 hr from a rat killed by an anesthetic overdose; PM delay of 3 hr, killed by decapitation; PM delay of 5 hr, killed by anesthetic overdose; and PM delay of 7 hr, killed by anesthetic overdose. Note that in the first four conditions large pyramidal cells have a similar appearance. After a PM delay of 7 hr, healthy cells were no longer observed.

The effects of various PM delays on the physiological state of the slice were then quantified by using two parameters. The first parameter was the average resting membrane potential of layer V pyramidal cells, which remained constant at PM delays of up to 9 hr (see Table 1). However, the number of cortical cells that could be recorded in PM slices diminished after 5–7 hr and no cell could be recorded after a PM delay of 12 hr. The second parameter was the field potential evoked by lateral olfactory tract stimulation in layer I of primary olfactory cortex slices. The afferent volley amplitude (reflecting the number of afferent fibers stimulated) and the dendritic excitatory postsynaptic potential (field EPSP, reflecting the number of synapses activated) increased with the stimulation intensity. The maximal field EPSP slope and the initial slope of the input/output curve (Table 1) remained constant at PM delays

Table 1. Influence of the PM delay on cell resting membrane potential and field potentials

PM delay, hr	Resting membrane potential, mV	Maximal field EPSP slope, mV/msec	Initial slope of the input/output curve, $msec^{-1}$
0	−74 ± 3 (9)	0.8 ± 0.4 (7)	1.6 ± 0.9 (7)
1	−76 ± 3 (10)	ND	ND
2	ND	0.6 ± 0.3 (6)	1.1 ± 0.8 (6)
3	−77 ± 1 (10)	ND	ND
5	ND	0.9 ± 0.5 (4)	1.2 ± 1 (4)
7	−75 ± 4 (10)	Not measurable, (4)	Not measurable (4)
9	−70 ± 6 (6)	Not measurable (4)	Not measurable (4)
12	Not measurable	ND	ND

Resting membrane potentials were determined from layer V pyramidal cells in neocortical slices. The maximal field excitatory postsynaptic potential (EPSP) slope was measured from the largest EPSP evoked in layer I of olfactory cortical slices by electrical stimulation of the lateral olfactory tract. The input/output curve was obtained by plotting EPSP slope as a function of the afferent volley amplitude. ND, not determined. All values are given as mean ± SD with n in parentheses.

of up to 5 hr. At a PM delay of 7 hr, barely any synaptic response was detected. These values of PM delay define a critical period lasting 5–6 hr, during which brain tissue is able to recover some neuronal activity.

To determine more precisely to what extent brain tissue from PM slices was "normal," we then analyzed neuronal intrinsic membrane properties. In the experiments described below, brain tissue was prepared after PM delays of 1–3 hr, although similar results were obtained with longer delays (5 hr). First, we performed an analysis of cell firing properties in various brain regions. In the neocortex, pyramidal cells from layers II-III and V showed typical morphological features and intrinsic membrane properties ($n = 15$) (14). Fig. 2A illustrates a layer V pyramidal cell recorded after a PM delay of 2 hr that displayed a spiking behavior, indicating the expression of normal voltage-dependent conductances. Similar firing properties were observed in CA1 hippocampal pyramidal cells ($n = 5$; not shown) (15). Interneurons, whether recorded in the neocortex ($n = 8$) (Fig. 2*D*) or in the hippocampus ($n = 4$) (not shown), displayed as expected various firing properties (12, 16, 17). In the thalamus, relay cells showed two types of firing (18): at depolarized potentials they fired tonically, whereas at hyperpolarized potentials they generated spike bursts due to a strong low-threshold calcium spike ($n = 6$; Fig. 2*B*). Purkinje cells recorded in PM cerebellar slices exhibited characteristic intrinsic membrane properties (19) such as delayed and anomalous rectification, plateau potentials (not shown), and sodium- and calcium-dependent action potentials ($n = 7$; Fig. 2*C*).

To investigate whether synaptic connections were still functional in PM neocortical slices, we recorded four neurons in voltage-clamp with patch pipettes containing CsCl and detected in each case spontaneous excitatory and inhibitory synaptic currents. As shown in Fig. 2*E*, bicuculline (a GABA A receptor antagonist) blocked the slowest spontaneous postsynaptic currents, whereas 6,7-dinitroquinoxaline-2,3-dione [DNQX; a glutamate α-amino-3-hydroxy-5-methyl-4-isoxazolepropionic acid (AMPA) receptor antagonist] blocked the fast excitatory postsynaptic currents. Evoked synaptic responses were similarly recorded in CA1 pyramidal cells ($n = 4$) and contained, as expected, an *N*-methyl-D-aspartate (NMDA) receptor component at depolarized membrane potentials (not shown) (20, 21). These results indicate that PM neurons express the same firing and synaptic properties as neurons from standard slices.

We then investigated the mRNA and protein expression in neurons after PM delays of 1–2 hr. In six neocortical inter-

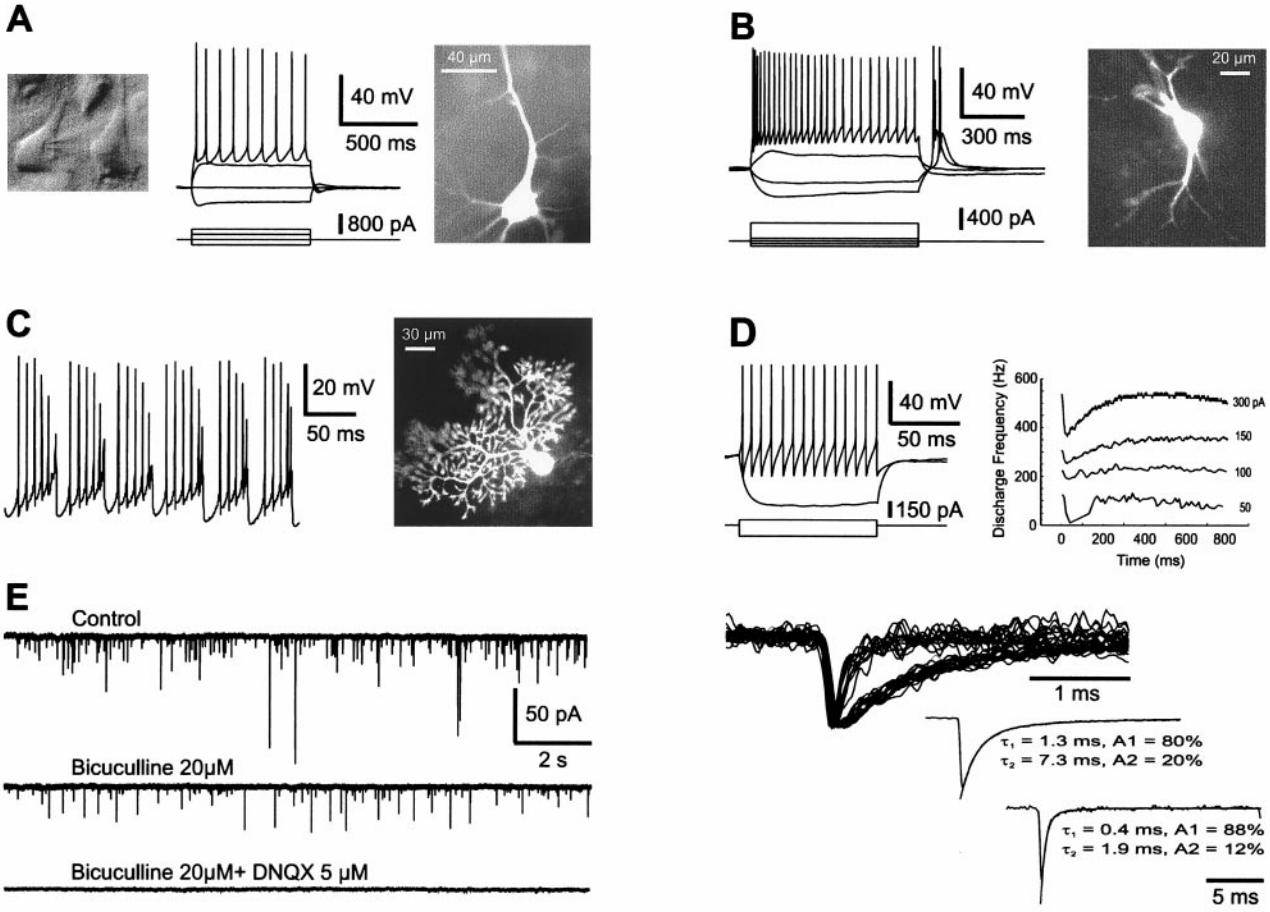

FIG. 2. Cell morphology, intrinsic membrane properties, and synaptic activity in PM rat brain slices. Recordings were obtained from both young ((*A–C, E*), 16/25-day-old) and adult (*D*) animals. (*A*) A neocortical pyramidal cell from layer V was visualized under infrared videomicroscopy (*Left*), recorded in whole-cell mode (*Center*; *Upper*, membrane potential, *Lower*, injected current) and loaded with biocytin (*Right*). Resting membrane potential, −71 mV, PM delay of 2 hr. (*B*) Firing properties (*Left*) and morphology (*Right*) of a thalamic relay cell that shows a typical low-threshold calcium spike at the end of a hyperpolarizing current pulse. Resting membrane potential, −71 mV; PM delay of 2 hr. (*C*) Burst firing behavior induced by steady depolarizing current (*Left*) in a cerebellar Purkinje cell labeled with biocytin (*Right*), PM delay of 90 min. (*D*) Firing properties of an adult neocortical interneuron (fast spiking) from layer II that was spontaneously active. The instantaneous frequency plot shows little accommodation (current pulses of + 50, 100, 150, and 250 pA); PM delay of 2 hr. (*E*) γ-Aminobutyric acid (GABA) A- and glutamate-mediated synaptic currents recorded in a layer V neocortical interneuron. The cell was voltage clamped at −71 mV and recorded with a pipette containing CsCl. (*Left*) The spontaneous synaptic currents (*Top*) were sensitive either to bicuculline (20 μM) or to 6,7-dinitroquinoxaline-2,3-dione (DNQX) (5 μM). (*Upper Right*) Selected synaptic currents to differentiate slow GABAergic from fast glutamatergic currents. (*Lower Right*) Both averaged synaptic current types were fitted with two exponentials.

neurons that were presumably GABAergic, whole-cell recordings were followed by aspiration of the cytoplasm, and the presence of mRNAs coding for the enzyme GAD was analyzed by using the single-cell RT-PCR technique (12). Fig. 3*A* shows a cortical interneuron from layer V that was characterized as a regular spiking cell and expressed mRNA coding for GAD_{65}. In all cases, GAD_{65} and/or GAD_{67} mRNAs could be detected, suggesting that mRNA is not degraded or is even synthesized PM.

To confirm the latter possibility, we investigated whether PM neurons were able to synthesize the immediate early gene protein c-Fos *de novo*. After PM delays of 1 or 2 hr, the dentate gyrus of hippocampal slices expressed c-Fos very weakly in control conditions (Fig. 3*B*). Stimulation of the slices with the glutamate agonist, kainic acid, alone ($n = 4$) or together with the GABA A receptor antagonist bicuculline ($n = 4$), or with a high $[K^+]_{external}$ solution ($n = 4$) strongly induced the synthesis of c-Fos. This effect was temperature-dependent: c-Fos synthesis was observed only when slices were heated at 35°C and not when they were maintained at room temperature. Induction of c-Fos was inhibited by blockers of transcription (actinomycin D, $n = 4$) and translation (cycloheximide, $n = 4$) demonstrating that mRNAs and proteins can be synthesized in PM slices. Thus, at the cellular level, neurons from standard or PM slices appear indistinguishable.

These observations led us to investigate the state of PM neuronal tissue in preparations that preserve the whole brain and better reflect *in vivo* conditions. First, the entire brain was anatomically screened for altered regions after a PM delay of 1 hr. We could not observe any difference in thionin-stained slices obtained from animals perfused and fixed either right after death or 1 hr later (not shown). We then recorded electrical activity in a modified isolated whole-brain preparation of the adult guinea pig (9). Animals ($n = 6$) were perfused transcardially for 3 min right after death with a standard oxygenated saline (20–24°C) to avoid blood clotting (this step was compulsory for subsequent recovery). After a delay of 1–2 hr, their brains were transferred to a recording chamber and arterially perfused with an oxygenated medium heated to 27–30°C. During the first 45–60 min of arterial perfusion no spontaneous or evoked electrical activity was recorded. After about 1 hr, evoked responses recovered, although the EEG remained isoelectric as in control isolated brains at the same temperature. Stimulation of the lateral olfactory tract induced characteristic field potential responses in the posterior piriform cortex (Fig. 4*A*) as reported *in vivo* and *in vitro* (22, 23). Current source density analysis of the evoked field potentials revealed the presence of two sinks (10). The first, located in lamina Ia, corresponds to the termination site of the lateral olfactory tract input and the second, recorded slightly deeper (layer Ib), is due to a disynaptic activation of layer II and III pyramidal cells (23). Stimulation of the lateral olfactory tract also evoked field potentials in the entorhinal cortex, the latency of the response being larger than in the piriform cortex ($n = 3$, Fig. 4*B Upper*). In the PM isolated whole brain, functional long-range synaptic connections were thus restored upon reoxygenation for more than 3–4 hr. This evoked neuronal population activity was corroborated by normal firing properties, as illustrated in Fig. 4*B Lower* by the discharge of a pyramidal cell recorded in the entorhinal cortex.

To induce network activity, we increased the extracellular K^+ concentration to 7.7 mM and added picrotoxin (200 μM),

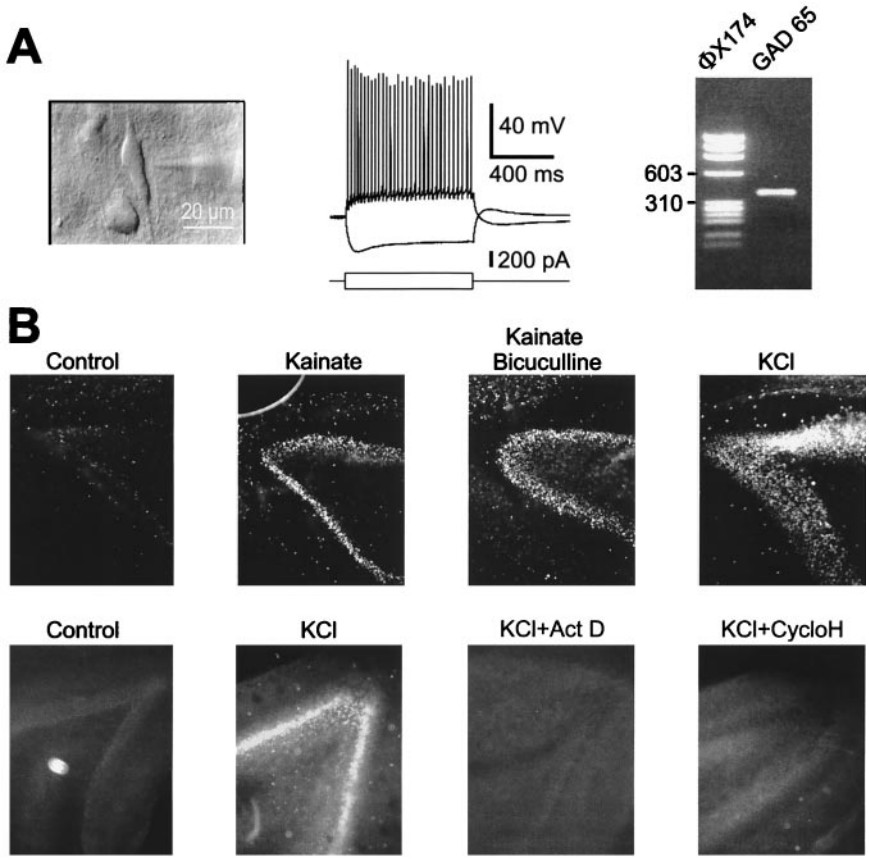

FIG. 3. mRNA expression and protein synthesis in PM neurons (PM delay of 1 hr). (*A*) A vertically oriented interneuron (*Left*) was recorded in layer V of a neocortical PM slice. This cell fired regularly (*Center*) and expressed GAD_{65} mRNAs (*Right*) as revealed by single-cell RT-PCR. Size markers from bacteriophage ϕX174 DNA are in the left lane. (*B*) (*Upper*) In PM hippocampal slices, synthesis of c-Fos in the dentate gyrus was induced by kainate (10 μM), kainate (10 μM)/bicuculline (20 μM), or by KCl (50 mM) and was revealed by immunocytochemistry. (*Lower*) Actinomycin D (5 μM) and cycloheximide (35 μM) blocked the induction of c-Fos by high K^+.

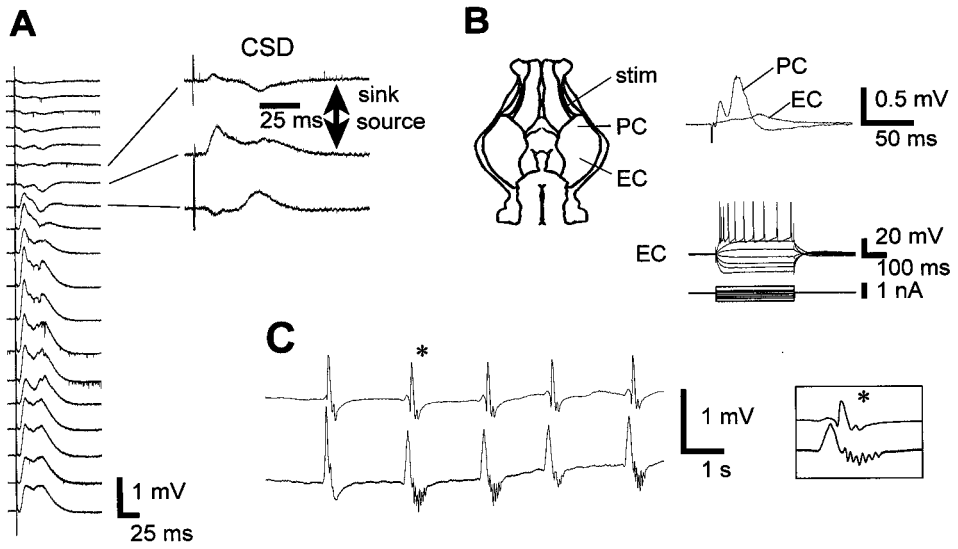

FIG. 4. Cell and network activity in the PM guinea pig. (*A*) Depth profile analysis in the posterior piriform cortex of an adult guinea pig whole brain *in vitro* reperfused after a PM delay of 90 min. (*Left*) Averaged field potentials ($n = 5$) recorded from surface (top) to interior (60-μm steps) in response to lateral olfactory tract stimulation. (*Right*) For three field potential traces, the corresponding current source density (CSD) traces are shown. Note the presence of two sinks, the superficial one corresponding to the termination site of the lateral olfactory tract input and the deeper one due to a disynaptic activation of layer II and III pyramidal cells. (*B*) (*Upper*) Stimulation of the lateral olfactory tract (stim) evoked synaptic responses in the posterior piriform (PC) and entorhinal (EC) cortices. (*Lower*) intrinsic membrane properties of a pyramidal cell (intracellular recording) in the EC. (*C*) In another guinea pig brain (PM delay of 75 min), raising the extracellular K^+ concentration to 7.7 mM and adding 200 μM picrotoxin induced bilateral spontaneous and synchronous epileptiform bursts in the temporal lobes.

a GABA A receptor antagonist that crosses the blood–brain barrier, to relieve inhibition ($n = 3$). Under these conditions, self-sustained rhythmic epileptiform discharges could be recorded bilaterally and synchronously in the temporal lobes (Fig. 4*C*). This epilepsy results from a reentrant loop activity in the hippocampal-entorhinal circuit (not shown) (24) and demonstrates that a major neuronal network can be activated in a PM brain.

DISCUSSION

Our study shows that after a complete interruption of cerebral blood flow, rat brain tissue is "physiologically" preserved *in situ* in a quiescent state, with no electrical activity for a critical period lasting 5–6 hr, during which it can be reactivated upon reperfusion. Reactivated brain tissue appears indistinguishable from standard tissue prepared immediately after death as far as the behavior of membrane channels and synaptic release machinery are concerned. It contains undegraded mRNAs and it is capable of protein synthesis. The duration of the critical period in rats delineates the maximal delay between cardiac arrest and attempt to reactivate tissue, provided that brain temperature declines normally after cardiac arrest. Our results thus differ from what has been previously assumed in *in vitro* studies, mainly that reducing the delay between decapitation and reoxygenation of brain slices was compulsory to preserve the tissue (7), although some have questioned this assumption (25, 26).

On the other hand, PM tissue cannot be defined as normal for two reasons. First, several aspects of its physiology were not investigated. Indeed, it is known that brain tissue reoxygenation after ischemia is associated with an increase in glutamate release (1, 27, 28), a rise in intracellular calcium (29, 30), selective gene activation (31, 32), and depression of protein synthesis and energy metabolism (5, 33). However, the drop in brain temperature occurring during cardiac arrest should prevent these mechanisms, which are highly temperature dependent (34–36). This drop of temperature is at least as fast as that which occurs during a four-vessel occlusion (0.5°C/min), during which a 2°C decrease in brain temperature has been shown to diminish dramatically the postischemic neuropathological outcome (37).

Second, brain tissue reactivation was studied only during the short recovery period imposed by the acute *in vitro* approach. Such short-term recovery does not preclude the occurrence of the processes cited above, as well as of delayed cell death, upon prolonged reactivation (2). Study of delayed damages would require keeping the tissue for at least 12–24 hr at 37°C, conditions that are difficult to achieve with slices prepared either in standard conditions or after various PM delays.

Are these results compatible with observations from larger intact mammals? In cats and monkeys, resuscitation has been achieved after 1 hr of complete circulatory arrest, although delayed lesions occur in vulnerable brain regions (3, 4). In humans, cardiac arrests of prolonged durations are tolerated in conditions of hypothermia, whether it is accidental (38) or controlled during cardiac surgery (39). However, in normothermic conditions, successful cardiac resuscitation is not obtained when circulatory arrest lasts more than a few minutes. This brief critical period differs markedly from that observed in rats, and the underlying causes of this difference remain to be established. Because we did not systematically examine the parameters controlling the duration of the critical period and because we could not investigate delayed postischemic damages, our results should not influence guidelines for resuscitation and transplantation procedures in humans. We nevertheless suggest that functional investigations for diagnostic purposes could be attempted in human brain tissue obtained during early autopsy.

We thank B. Cauli and F. Debarbieux for their help with the PCR amplification and the immunocytochemistry, and J. Rossier for his constant support. We particularly appreciated the critical comments of J. Rossier, P. Ascher, M. Scanziani, and J. Brunton.

1. Meldrum, B. & Garthwaite, J. (1990) *Trends Pharmacol. Sci.* **11,** 379–387.
2. Choi, D. W. (1996) *Curr. Opin. Neurobiol.* **6,** 667–672.
3. Hossmann, V. & Hossmann, K. A. (1973) *Brain Res.* **60,** 423–438.
4. Hossmann, K. A. & Zimmermann, V. (1974) *Brain Res.* **81,** 59–74.

5. Hossmann, K. A. (1993) *Prog. Brain Res.* **96,** 161–177.
6. Kleihues, P. & Hossmann, K. A. (1973) *Acta Neuropathol. (Berlin)* **25,** 313–324.
7. Aitken, P. G., Breese, G. R., Dudek, F. F., Edwards, F., Espanol, M. T., Larkman, P. M., Lipton, P., Newman, G. C., Nowak, T. S., Jr., Panizzon, K. L., *et al.* (1995) *J. Neurosci. Methods* **59,** 139–149.
8. Horikawa, K. & Armstrong, W. E. (1988) *J. Neurosci. Methods* **25,** 1–11.
9. Mühlethaler, M., de Curtis, M., Walton, K. & Llinas, R. (1993) *Eur. J. Neurosci.* **5,** 915–926.
10. Nicholson, C. & Freeman, J. A. (1975) *J. Neurophysiol.* **38,** 356–368.
11. Lambolez, B., Audinat, E., Bochet, P., Crepel, F. & Rossier, J. (1992) *Neuron* **9,** 247–258.
12. Cauli, B., Audinat, E., Lambolez, B., Angulo, M.-C., Ropert, N., Tsuzuki, K., Hestrin, S. & Rossier, J. (1997) *J. Neurosci.* **17,** 3894–3906.
13. Zhang, X., Le Gal La Salle, G., Ridoux, V., Yu, P. H. & Ju, G. (1997) *Eur. J. Neurosci.* **9,** 29–40.
14. Connors, B. W. & Gutnick, M. J. (1990) *Trends Neurosci.* **13,** 99–104.
15. Brown, D. A., Gahwiler, B. H., Griffith, W. H. & Halliwell, J. V. (1990) *Prog. Brain Res.* **83,** 141–160.
16. Buhl, E. H., Han, Z. S., Lorinczi, Z., Stezhka, V. V., Karnup, S. V. & Somogyi, P. (1994) *J. Neurophysiol.* **71,** 1289–1307.
17. Buhl, E. H., Szilagyi, T., Halasy, K. & Somogyi, P. (1996) *Hippocampus* **6,** 294–305.
18. Llinas, R. & Jahnsen, H. (1982) *Nature (London)* **297,** 406–408.
19. Llinas, R. & Sugimori, M. (1980) *J. Physiol. (London)* **305,** 171–195.
20. Collingridge, G. L., Herron, C. E. & Lester, R. A. (1988) *J. Physiol. (London)* **399,** 283–300.
21. Nowak, L., Bregestovski, P., Ascher, P., Herbet, A. & Prochiantz, A. (1984) *Nature (London)* **307,** 462–465.
22. de Curtis, M., Pare, D. & Llinas, R. R. (1991) *Hippocampus* **1,** 341–354.
23. Rodriguez, R. & Haberly, L. B. (1989) *J. Neurophysiol.* **61,** 702–718.
24. Pare, D., deCurtis, M. & Llinas, R. (1992) *J. Neurosci.* **12,** 1867–1881.
25. Leonard, B. W., Barnes, C. A., Rao, G., Heissenbuttel, T. & McNaughton, B. L. (1991) *Exp. Neurol.* **113,** 373–377.
26. Ragsdale, D. S. & Miledi, R. (1991) *Proc. Natl. Acad. Sci. USA* **88,** 1854–1858.
27. Benveniste, H., Drejer, J., Schousboe, A. & Diemer, N. H. (1984) *J. Neurochem.* **43,** 1369–1374.
28. Rothman, S. M. (1983) *Science* **220,** 536–537.
29. Araki, T., Kato, H. & Kogure, K. (1990) *Brain Res.* **528,** 114–122.
30. Kass, I. S. & Lipton, P. (1986) *J. Physiol. (London)* **378,** 313–334.
31. Nowak, T. S., Jr., Osborne, O. C. & Suga, S. (1993) *Prog. Brain Res.* **96,** 195–208.
32. Abe, K. & Kogure, K. (1993) *Prog. Brain Res.* **96,** 221–236.
33. Kleihues, P. & Hossmann, K. A. (1971) *Brain Res.* **35,** 409–418.
34. Dietrich, W. D., Busto, R., Globus, M. Y. & Ginsberg, M. D. (1996) *Adv. Neurol.* **71,** 177–194; discussion 194–197.
35. Globus, M. Y., Busto, R., Dietrich, W. D., Martinez, E., Valdes, I. & Ginsberg, M. D. (1988) *J. Neurochem.* **51,** 1455–1464.
36. Welsh, F. A., Sims, R. E. & Harris, V. A. (1990) *J. Cereb. Blood Flow Metab.* **10,** 557–563.
37. Busto, R., Dietrich, W. D., Globus, M. Y., Valdes, I., Scheinberg, P. & Ginsberg, M. D. (1987) *J. Cereb. Blood Flow Metab.* **7,** 729–738.
38. Walpoth, B. H., Walpoth-Aslan, B. N., Mattle, H. P., Radanov, B. P., Schroth, G., Schaeffler, L., Fischer, A. P., von Segesser, L. & Althaus, U. (1997) *N. Engl. J. Med.* **337,** 1500–1505.
39. Griepp, E. B. & Griepp, R. B. (1992) *J. Cardiovasc. Surg.* **7,** 134–155.